Atmos. Chem. Phys., 23, 2235–2249, 2023
https://doi.org/10.5194/acp-23-2235-2023

Atmospheric Chemistry and Physics
Open Access
EGU

Insoluble lipid film mediates transfer of soluble saccharides from the sea to the atmosphere: the role of hydrogen bonding

Minglan Xu, Narcisse Tsona Tchinda, Jianlong Li, and Lin Du

Environment Research Institute, Shandong University, Binhai Road 72, Qingdao 266237, China

Correspondence: Lin Du (lindu@sdu.edu.cn)

Received: 5 September 2022 – Discussion started: 23 September 2022
Revised: 13 January 2023 – Accepted: 1 February 2023 – Published: 15 February 2023

Abstract. Saccharides are a large portion of organic matter in sea spray aerosol (SSA). Although they can affect climate-related properties of SSA, the mechanism through which saccharides are transferred from bulk seawater to the ocean surface and ultimately into SSA is still debated. Here, the transfer of small soluble saccharides was validated using a controlled plunging jet sea spray aerosol generator to better understand the wide range of particle properties produced by natural seawater mixed with model organic species, glucose and trehalose. We showed that both soluble saccharides can promote the production of SSA particles, and the presence of trehalose could increase the SSA number concentration by 49.4 %. Conversely, the role of the insoluble fatty acid film on the seawater surface greatly reduced the production of SSA. The resulting inorganic–organic mixed particles identified by the transmission electron microscope (TEM) showed typical core–shell morphology. A Langmuir model was used to parameterize the adsorption and distribution of saccharide into SSA across the bubble surface, while infrared reflection–absorption spectroscopy (IRRAS) combined with Langmuir isotherms was undertaken to examine the effects of aqueous subphase soluble saccharides with various concentrations on the phase behavior, structure, and ordering of insoluble lipid monolayers adsorbed at the air/water interface. We found that the adsorption of glucose and trehalose on the fatty acid monolayer led to the expansion of the mean molecular area. Saccharide–lipid interactions increased with increasing complexity of the saccharide in the order of glucose $<$ trehalose. In a seawater solution, the effects of dissolved saccharides on the ordering and organization of fatty acid chains were muted. The enhancement of the carbonyl band to the low wavenumber region implied that soluble saccharides can form new hydrogen bonds with fatty acid molecules by displacing large amounts of water near the polar headgroups of fatty acids. Our results indicate that the interaction between soluble saccharides and insoluble fatty acid molecules through hydrogen bonds is an important component of the sea–air transfer mechanism of saccharides.

1 Introduction

Sea spray aerosol (SSA) represents a major source of aerosol particle populations and significantly impacts the Earth's radiation budget, cloud formation, and microphysics, by serving as cloud condensation nuclei (CCN) and ice nuclei (IN), and microbial cycling (Bertram et al., 2018; Partanen et al., 2014). The formation of SSA particles is strongly influenced by the uppermost sea surface microlayer (SML), which is a thin layer of 1–1000 µm thickness formed due to different physico-chemical properties of air and seawater (Wurl et al., 2017). Beyond sea salt, the ocean surface contains a fair amount of organic matter (OM) mass fraction, covering carbohydrates, lipids, proteins, humic-like substances (HULIS), intact phytoplankton cells and fragments, fungi, viruses, and bacteria (Van Pinxteren et al., 2020; Cunliffe et al., 2013). This organic matter coincides with some chemical markers that are enriched in the SSA, which is mainly produced by bubble mediation (Russell et al., 2010; Facchini et al., 2008). When a bubble reaches the water surface, destroy-

ing the surface membrane of the water, the bubble bursts into many so-called film drops. After the bubble film breaks, a jet of water rising vertically from the ruptured bubble cavity forms so-called jet drops. Film drops are responsible for the major proportion (∼ 60 %–80 %) of submicron particles, whereas jet drops contribute significantly to the production of supermicron particles (Wang et al., 2017). Both the size and chemical composition of SSA are important properties in determining cloud formation and eventually radiative forcing (Brooks and Thornton, 2018). Hence, understanding the physico-chemical mechanisms driving these variations is essential for predicting SSA composition and climate-related processes.

Surface-active biomolecules are preferentially transferred from marine surface water into the atmosphere through the bubble-bursting processes, forming a considerable fraction of primary marine organic aerosols (Schmitt-Kopplin et al., 2012). Previous measurements have shown that up to 60 % of ocean particle mass can be organic, which exhibits a strong size dependence (O'Dowd et al., 2004; Russell et al., 2010). Spectroscopic evidence from field-collected SSA particles indicates that the oxygen-rich organic fractions of individual particles contain molecular signatures of saccharides and carboxylic acids (Hawkins and Russell, 2010). For example, it has previously been observed that the carbohydrate-like spectroscopic signatures account for 40 %–61 % of the submicron SSA organic mass (Quinn et al., 2014; Russell et al., 2010). A large portion of this mass is attributed to saccharides that are transferred from seawater to SSA, and it shows a certain enrichment in SSA. Specifically, the high enrichment factor of carbohydrates was calculated for supermicron (20–4000) and submicron (40–167 000) particles relative to the bulk seawater in the Western Antarctic Peninsula (Zeppenfeld et al., 2021). According to previous laboratory studies, marine bacteria, divalent cations, and protein can affect the saccharide enrichment in SSA (Hasenecz et al., 2020; Schill et al., 2018). However, a mechanistic and predictable understanding of these complex and interacting processes in favor of saccharides found in marine aerosol particles remains largely unexplored, despite their oceanic and atmospheric significance.

A variety of saccharides have been found ubiquitously in the ocean, including dissolved free monosaccharides, oligo/polysaccharides, sugar alcohols, and monosaccharide dehydrates, the composition of which depends on marine biological activity (Van Pinxteren et al., 2012). Frossard et al. (2014) used the hydroxyl characteristic functional group of atmospheric marine aerosols from Fourier transform infrared spectroscopy to infer the contributions of different saccharides in SSA. It was found that the primary marine aerosols produced in biologically productive seawater had a stronger hydroxyl group characteristic of monosaccharides and disaccharides, while the hydroxyl groups of seawater organic matter were closer to those of polysaccharides. This suggests that larger saccharides may be preferentially retained in seawater during aerosol production. An analysis of aerosol samples collected on the Western Antarctic Peninsula also showed that not only polysaccharides but also a high portion of free monosaccharides mainly composed of glucose, fructose, rhamnose, and glucosamine were present (Zeppenfeld et al., 2021). Raman spectroscopy was used to measure individual SSA particles generated via wave-breaking in a wave flume under algal bloom conditions to get a deeper insight into their organic categories. It was reported that 4 %–17 % and 3 %–46 % of sub- and supermicron particles show strong spectral characteristics of free saccharides and short-chain fatty acids, respectively (Cochran et al., 2017). However, current climate models largely underestimate the ratio of saccharides in marine aerosols (Cravigan et al., 2020), and there is an urgent need to clarify the physico-chemical mechanisms that drive saccharides transfer to SSA.

A possible explanation for the origin of saccharides in SSA chemical composition involves the affinity between the bulk aqueous soluble saccharides and insoluble surfactant monolayers already adsorbed at the air/water interface, resulting in co-adsorption of the soluble saccharides (Link et al., 2019b). This co-adsorption arises from non-covalent interactions and promotes the binding of soluble organic matter to the surface with insoluble Langmuir film. Previous studies have indicated that the presence of lipids or proteins strongly enhances the surface adsorption capacity of saccharides, even for highly soluble saccharides that do not adsorb individually at the air/water interface (Pavinatto et al., 2007; Burrows et al., 2016). For example, recent studies have shown that simple, soluble biomolecules such as phenylalanine and trehalose exhibit an affinity for lipid films, altering membrane permeability and phase behavior (Perkins and Vaida, 2017; Link et al., 2019a). A divalent cation-mediated co-adsorption mechanism was also proposed to explain the enrichment of monosaccharide in laboratory-generated SSA (Schill et al., 2018). Alternatively, saccharides can be bound covalently to larger, more surface-active biomolecules, such as glycoproteins or lipopolysaccharides, which attach to SML and are eventually transferred into SSA through bubble bursting at the ocean surface (Estillore et al., 2017). Although different hypotheses have been proposed, there is still debate about the more nuanced mechanisms that guide the sugar–lipid interactions in the marine environment.

The present work aims to use a multi-pronged approach that combines bulk SSA production experiments, Langmuir surface pressure-area isotherms, and infrared reflection–absorption spectroscopy (IRRAS) to examine the role of saccharides in SSA production and the mechanism of saccharides transfer and enrichment from aqueous solution into SSA. The study focuses on two soluble saccharides that are prevalent in seawater, glucose and trehalose, which are uncharged monosaccharides and disaccharides, respectively. A plunging jet sea spray aerosol generator was used to generate nascent SSA particles by artificially generating bubbles in seawater as a mean of simulating sea spray production by

breaking waves. This simulation helps evaluate the impact of soluble saccharides and insoluble fatty acids on SSA production and particle morphology. Langmuir isotherms provided abundant information for stability and fluidity of monolayers, which were used to adequately describe the magnitude of interaction effects between subphase soluble saccharides and surface insoluble surfactants. Finally, IRRAS spectra provided molecular-scale descriptions of monolayer conformational information and allowed us to deduce the distribution of saccharide species at the interface. By combining all the findings, we propose a model of sea–air transfer of marine saccharides through hydrogen bond interactions involved in surface insoluble lipid molecules.

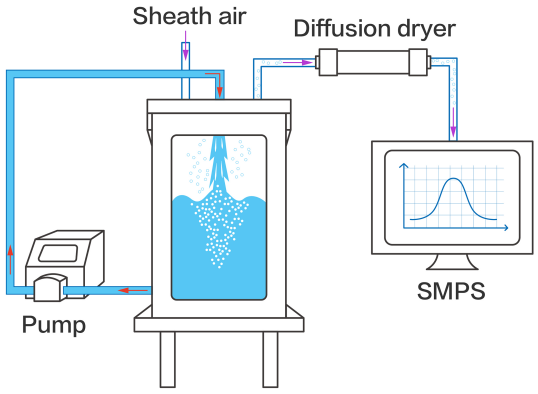

Figure 1. Schematic picture of the plunging jet sea spray aerosol generator. The red arrows represent the flow direction of seawater, and the purple arrows represent the flow of gases and aerosols.

2 Experimental sections

2.1 Materials and solutions

D-(+)-glucose (Glu, powder, $\geq 99.5\,\%$) and D-(+)-trehalose anhydrous (Tre, powder, 99 %) were purchased from Aladdin. Stearic acid (SA, $> 98\,\%$, TCI), palmitic acid (PA, $> 98\,\%$, Adamas-Beta), and myristic acid (MA, $\geq 99.5\,\%$, Aladdin) were prepared in chloroform (AR, $\geq 99.0\,\%$, Sinopharm Chemical Reagent Co., Ltd.) at a final concentration of 1 mM each. Figure S1 in the Supplement shows the chemical structures of the three fatty acids used in this study. The respective fatty acid solutions were mixed at a molar ratio of 2 MA : 4 PA : 3 SA to obtain a mixed lipid stock solution considering that PA and SA account for approximately two-thirds of the total saturated fatty acids in fine SSA particles, with MA being the third most abundant species (Cochran et al., 2016). All chemicals were used without further purification. The natural seawater (SW) was collected from Shazikou, Qingdao, China. Here, surface seawater (within 0.1–1 m below the sea surface) was obtained from a pier on the coast by immersing high-density polyethylene containers into the water. The sampled seawater was microfiltered through a 0.2 µm polyethersulfone filter (Supor®-200, Pall Life Sciences, USA) to remove large particles such as sediments, algae, and bacteria. The filtered seawater was used for SSA generation and as a filling subphase for interfacial experiments. The pH of natural seawater, initially determined to be about 8.13 ± 0.02, was measured to be around 8.04 ± 0.01 at the end of the experiment. Different concentrations of saccharide-containing seawater solutions required in the experiments were obtained by dissolving different masses of glucose or trehalose in the filtered natural seawater using mechanical stirring.

2.2 SSA production and collection

SSAs were produced using a plunging jet sea spray aerosol generator (Fig. 1). A physical drawing of the aerosol generation system can be found in Fig. S2. The generator and its detailed operation principle has been described elsewhere (Liu et al., 2022). Briefly, the generator consists of a stainless steel (shipboard class, 316 L) rectangular sealed container and a viewable glass window. The upper removable lid has ports for water inlet, purging air, and sampling. The purge air is supplied by a zero-air generator (Model 111, Thermo Scientific, USA) and the flow rate is controlled at $10\,\mathrm{L\,min^{-1}}$. A peristaltic pump (WL600-1A, ShenChen) periodically circulates water from the bottom of the generator to the top nozzle through a Teflon tube with a pump speed of $1\,\mathrm{L\,min^{-1}}$, creating a plunging water column that hits the seawater surface and entrains air into the bulk seawater. The bubble plumes extend approximately 15 cm down into the water, a moderate depth considering that the majority of the air being entrained is located within about 50 cm from the sea surface (Hultin et al., 2010). When the bubbles rise to the air/water interface and burst, they generate SSA emissions. When studying insoluble surfactant effects, a concentrated solution of 1 mM mixed fatty acids in chloroform was added to the surface of the seawater solution. After the necessary fatty acids were added, only the sheath air flowed, allowing the chloroform to evaporate for 15 min and leaving only the surfactant on the surface. After pre-preparation for 15 min, the sheath air and peristaltic pump were turned on to produce SSAs. Prior to collection, SSAs were dried to a relative humidity of $\sim 40\,\%$ using a diffusion dryer. Thereafter, a scanning mobility particle sizer (SMPS, model 3936, TSI) consisting of a differential mobility analyzer (DMA, model 3081, TSI Inc., USA) and a condensation particle counter (CPC, model 3776, TSI Inc., USA) was used to measure the particle size distributions and number concentrations. The particle size distribution ranging from 13.6 to 710.5 nm was obtained at a sheath flow rate of $3.0\,\mathrm{L\,min^{-1}}$ and an aerosol flow rate of $0.3\,\mathrm{L\,min^{-1}}$. Dried SSAs were deposited onto 200 mesh copper grids with carbon foil (T11023, Tilan, China) by a single particle sampler (DKL-2, Genstar electronic technology Co., Ltd.) to further characterize the particle morphology.

2.3 Langmuir monolayer preparation and Langmuir isotherms

The Langmuir trough setup has been described previously (Xu et al., 2021). Briefly, it consists of a rectangular Teflon trough (Riegler & Kirstein, Germany) and two moveable Teflon barriers whose movements are precisely controlled to achieve symmetric compression of the monolayer at the air/water interface. A Wilhelmy plate attached to the pressure sensor was used to measure the surface pressure. Each 100 mL subphase consisted of natural seawater, with varying amounts of glucose or trehalose. Aliquots of mixed fatty acids stock solution were spread onto the subphase surface dropwise with a glass micro-syringe, and 15–20 min was allowed for the solvent to evaporate completely. The surface pressure (π), given by Eq. (1) and defined as the difference in surface tension between the pure air/water interface (γ_0) and the monolayer covered interface (γ), was monitored.

$$\pi = \gamma_0 - \gamma. \quad (1)$$

The barriers were compressed at a rate of 3 mm min^{-1} per barrier, and isotherm data were collected for surface pressure π (mN m^{-1}) versus area per molecule ($\mathrm{Å}^2$). All experiments were performed at (22 ± 3) °C and at relative humidity below 65 %.

2.4 Infrared reflection–absorption spectroscopy measurement

The polarization-modulation infrared reflection–absorption spectroscopy (PM-IRRAS) is a mainstream spectroscopic method for in situ characterization of Langmuir monolayers at the molecular level. For IRRAS spectra, floating monolayers were spread at the aqueous subphase and compressed to the desired surface pressure and stopped before obtaining the spectra. PM-IRRAS spectra were obtained using a Fourier transform infrared (FT-IR) spectrometer (Bruker Vertex 70, Germany) equipped with an external reflection accessory (XA-511). The interference infrared beam was set out from FT-IR and polarized by a ZnSe polarizer to alternately generate S- and P-polarization lights. They were then continuously modulated by a photo-elastic modulator (PEM-100) at a high frequency of 42 kHz to measure the spectra of both polarizations simultaneously. The infrared beam was focused onto the Langmuir film through a gold mirror, and then a portion of reflected light was directed onto the liquid nitrogen-cooled mercury–cadmium–telluride (MCT) detector. The application of polarization modulation attenuates the noise of reflective FT-IR and the interference of water vapor and carbon dioxide. The spectra presented here are reflectance–absorbance (RA) given as

$$\mathrm{RA} = -\log(R/R_0), \quad (2)$$

where R and R_0 are the reflectance of fatty acid monolayer and pure seawater solution surface, respectively. To obtain a better signal-to-noise ratio, spectra were collected with 2000 scans and 8 cm^{-1} resolution at a fixed incidence angle of 40°. To better compare the variation in the spectral region of interest, peaks were fitted to Gaussian functions using Origin 2021 for each displayed spectrum.

2.5 Transmission electron microscope imaging

Particle imaging was performed using a transmission electron microscope (TEM, FEI Tecnai G2 F20, FEI, USA) equipped with a Schottky field emission gun. It was operated at an accelerated voltage of 200 kV with a high angle annular dark field detector to collect TEM images and even preserve the soft internal structure of organic sources under high vacuum conditions.

3 Results and discussion

3.1 SSA particle number size distributions

To examine the sea–air transfer of soluble saccharides and their interaction with insoluble fatty acids, SSA particle generation experiments were carried out with seawater containing 1.0 g L^{-1} glucose or trehalose. Figure 2 shows the particle number size distributions resulting from seawater to which different soluble saccharides were added in the presence or absence of fatty acids on the surface. As a reference, the particle size distribution produced from natural seawater is also given. The submicron particle size distributions produced by the plunging jet generator are well represented by lognormal mode. In the absence of saccharides, a broad, unimodal mode of the particle size distribution around 168 nm was generated. This observation agrees quite well with a previous study that produced SSA by the plunging jet method with the mode of the particle size distribution $\sim$ 162 nm (Christiansen et al., 2019). Moreover, the SSA yielded by the plunging waterfall also has a size distribution similar to that yielded by the breaking wave, which has a particle number size distribution of $\sim$ 162 nm (Prather et al., 2013). This contrasts with most previous laboratory studies using sintered glass filters or frits, which tend to exhibit a smaller mean diameter and narrower distribution. This may be expected given that similar bubble size distributions exist in the two generation mechanisms using plunging waterfalls and breaking waves. A previous study using plunging jets has produced similar bubble size distributions (Fuentes et al., 2010). Importantly, the measured bubble spectrum for the breaking waves matches the shape and Hinze scale of the bubble spectra of the previously measured open ocean breaking waves (Deane and Stokes, 2002). Although we did not directly measure the bubble spectra generated by the plunging jet method in this study, it should be able to better simulate the properties of breaking waves according to the above empirical studies. Moreover, we compared the particle size distributions of SSA generated in our laboratory with those measured in field stud-

ies (Quinn et al., 2017; Xu et al., 2022). As shown in Fig. S3, it was observed that the size distribution of both laboratory-generated SSAs and SSAs measured in the field had a major accumulation mode in the range of ∼ 111–172 nm. However, the number concentration of SSAs produced in our experiment is about 2 orders of magnitude higher than that in the real environment. As a result, the jet sea spray generator system is capable of a wide range of measurements (e.g., size-resolved hygroscopicity and heterogeneous reactivity) that are not achievable at low number concentrations.

Laboratory studies of the effects of saccharide organic substances on droplet production have been inconclusive. A previous study has used two bubble generation methods (plunging water jet and diffusion aeration) to investigate the number size distribution of SSA particles produced, by mixing fructose and mannose with NaCl or artificial seawater solution (King et al., 2012). The results showed that the number concentration of particles produced by artificial seawater containing sodium dodecyl sulfate was significantly lower than that of particles produced by artificial seawater containing fructose. However, the NaCl solution containing mannose produced SSA with a lower number concentration than the NaCl solution containing sodium laurate. Lv et al. (2020) found that the addition of fructose to the sea salt solution can significantly promote the increase of the SSA number concentration. However, the above studies lacked direct comparative results on SSA production influenced by different soluble saccharides. For the plunging jet, our measurements indicate that soluble saccharides can promote the production of SSA to varying degrees. The number concentration, mass concentration, and geometric mean diameter are shown in the Supplement (see Table S1 for further details). It was observed that glucose led to a slight increase of about 15.6 % in particle number concentration, increasing the mode diameters to ∼ 175 nm. In contrast, the natural seawater spiked with trehalose resulted in a higher total particle number concentration that increased by approximately 49.4 % over a wide size range. Therefore, the changes in production and properties of SSA from actual seawater may be more complicated under the influence of different saccharides.

The effect of the interaction of insoluble fatty acids with different saccharides on SSA particles was investigated by spreading insoluble fatty acids on the seawater surface. In plain sight, fatty acids on the surface can significantly reduce the number concentration of SSA regardless of the presence of saccharides in the seawater. When the fatty acid surfactant was added to seawater alone, the number concentration decreased by about 17.2 %, while the presence of glucose resulted in a decrease of about 21.6 %. Moreover, fatty acids showed the highest inhibitory effect on SSA produced by trehalose-containing seawater solution, whose concentration decreased by about 49.4 %. We infer that the surface layer is significantly more stable in the presence of fatty acids, even when disturbed by the plunging jet, thus resulting in less bubble bursting. Furthermore, the continuous plunging caused

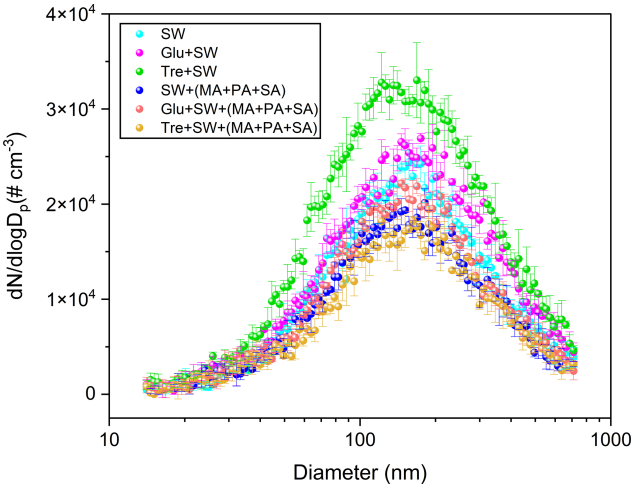

Figure 2. The particle number size distribution spectra of SSAs produced from a blank seawater sample and a seawater sample spiked with glucose or trehalose. Both results are presented here with and without fatty acid surface films.

a layer of foam to accumulate on the surface of the water. The presence of the foam layer on the seawater surface may be capable of prohibiting the production of droplets by assimilating rising bubbles into the foam layer before bursting. Collectively, the observed variability in these experiments suggests an urgent need to better build the link between total SSA particle flux and seawater organic composition over the ocean. However, sole bulk-phase generation experiments may not accurately capture the relevant chemical behaviors and support mechanism analysis that occur in the SML. Therefore, we attempted to explore the possible interaction mechanisms via air/water interface chemical experiments.

3.2 π-A isotherms of fatty acid monolayers

In this section, we only discuss traditional Langmuir monolayers, which operate on air/water interfaces that are ubiquitous along the sea surface (Elliott et al., 2014). The π-A isotherm reflects information on the phase behavior of the monolayer as a function of lipid packing density. As shown in Fig. 3, the π-A isotherms of individual and mixed fatty acids on the natural seawater subphase are presented. When the mechanical barriers initially begin to compress, the amphiphilic molecules in the monolayer are in the gaseous (G) phase under a large area per molecule, with the hydrophobic tails having significant contact with the water surface but little contact with each other. At this stage, the compression of the film does not lead to a significant change in surface pressure. As the monolayer is compressed, the intermolecular distances gradually decrease and the surface pressure begins to rise from zero into the liquid expanded (LE) phase, where the hydrophobic tails start to touch each other but re-

main largely disordered and fluid. This is represented as the lift-off area of the isotherm. Further compression results in a thermodynamic transition to a liquid condensed (LC) phase. The film is eventually compressed to a limiting point where the monolayer collapses as the materials leave the 2D film (Lee, 2008). In general, the collapse is an irreversible process, and the collapsed material does not reintegrate into the monolayer as the surface pressure decreases.

Although the π-A isotherms of individual fatty acids have been well studied, the phase behavior of the mixed binary and ternary systems still needs to be explored. Pure natural seawater, without spreading surface-active fatty acids, does not cause observable changes in the surface pressure, indicating that surface-active impurities are either absent or have too low concentrations to cause film formation. When myristic acid spreads on the water surface, it undergoes a long liquid phase, with a lower collapse pressure of $\sim 27\,\mathrm{mN\,m^{-1}}$ and an area per molecule as low as 5 $\mathrm{Å}^2$. This is due to the relatively high solubility of MA molecules in the aqueous phase, resulting in a large loss of molecules in the monolayer under the mechanical forcing from lateral barrier compression. In addition, according to the surface pKa value of 7.88 at 20 °C, MA is mostly deprotonated at pH $\sim$ 8.1, so a stable monolayer cannot be obtained for the natural seawater subphase due to the dissolution phenomenon (Carter-Fenk and Allen, 2018). For the palmitic acid monolayer, it goes through a relatively short gaseous phase and rapidly enters the liquid phase. After experiencing a kink point at $\sim 48\,\mathrm{mN\,m^{-1}}$, it continues to rise to the maximum surface pressure of $\sim 57\,\mathrm{mN\,m^{-1}}$ and collapses. Both the lift-off area and molecular area of the stearic acid film decreased more than those of the palmitic acid film. This is caused by the fact that the interaction (van der Waals force) between the molecules increases as the molecular weight of the long chain fatty acid increases. That is, increased attraction leads to a decrease in distance between SA molecules.

When fatty acids are mixed in a certain molar ratio and spread onto the interface water, it is found that the π-A isotherm lies between the pure fatty acids and is closer to that of stearic acid, but the mean molecular area is relatively smaller. The partial dissolution of myristic acid most likely accounts for the smaller mean molecular area observed in the proxy mixture isotherm compared to the palmitic acid and stearic acid isotherms. Moreover, we found that the π-A isotherms of mixed fatty acids exhibit similar collapsing behavior to those of stearic acid and palmitic acid at a surface pressure of about $50\,\mathrm{mN\,m^{-1}}$. Consequently, the longer fatty acids will dominate the lateral interactions of the SSA membrane, which makes the membrane more rigid due to the larger sum of diffusive interactions. In view of the true proportion of fatty acids in the nascent sea spray particles, we used a ternary fatty acid membrane proxy system composed of MA, PA, and SA (2 : 4 : 3 molar ratio) in the following experiments involving Langmuir isotherms.

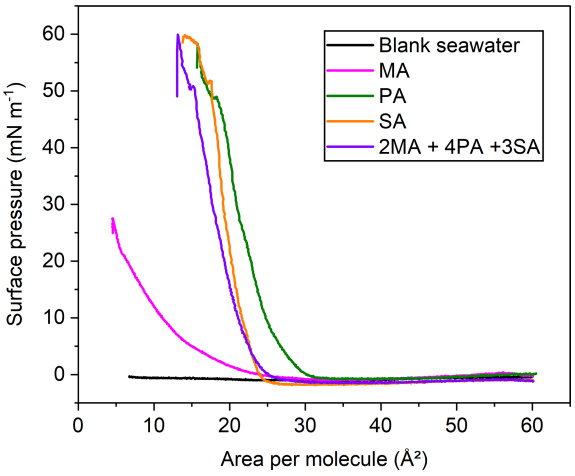

Figure 3. π-A isotherms of myristic acid, palmitic acid, stearic acid, and mixed fatty acids. The black trace represents the background natural seawater solution with no fatty acid spread.

3.3 Effect of soluble saccharides on the phase behavior of mixed monolayers

An effective way to test whether soluble saccharides associate with lipid membranes is to examine the effect of these saccharides on the phase behavior of lipid films. The π-A isotherms provide insights into the overall monolayer structure, intermolecular interactions, and the adsorption of glucose and trehalose. Both glucose and trehalose are highly soluble ($> 1.0\,\mathrm{g\,L^{-1}}$) in water. However, this solubility does not preclude their presence on the surface. According to some previous studies, the dissolved organic carbon concentration is about 0.7–1.0 mg carbon $\mathrm{L^{-1}}$ (Quinn et al., 2015; Hasenecz et al., 2019). Considering that saccharides in the ocean represent approximately 20 % of the dissolved organic carbon (Pakulski and Benner, 1992; Hasenecz et al., 2019), the saccharide concentration is about 0.14–0.20 mg $\mathrm{L^{-1}}$. The glucose and trehalose concentrations used for the π-A isotherms are approximately 3–4 orders of magnitude greater than the saccharide concentration in dissolved organic matter, maintaining detectivity within the π-A isotherms. Furthermore, high concentrations used here are still relevant, considering the evaporation process in aged sea spray aerosols (Hasenecz et al., 2020). At the same time, such concentrations are close enough to understand the enrichment of saccharides in the sea surface microlayer and to provide a confident interpretation of the physico-chemical mechanisms driving the adsorption and transfer of soluble saccharides (De Vasquez et al., 2022).

Figure 4 shows the π-A isotherms of mixed fatty acids on natural seawater subphases containing different concentrations (varied between 0.1 and 5.0 $\mathrm{g\,L^{-1}}$) of glucose or trehalose. In this case, the surface pressure and mean molecular area of the fatty acid monolayer is equal to that of the fatty acid monolayer with the addition of saccharides, provided

that the saccharide molecules do not affect the monolayer. At a low concentration of 0.1 g L^{-1}, both saccharides had little overall effect on the phase behavior of fatty acid monolayers. However, they resulted in a smaller lift-off area for the monolayer compared to pure natural seawater. As the glucose and trehalose subphase concentration increases, the monolayers are expanded, taking up a larger mean molecular area, which is consistent with previous research (Crowe et al., 1984). This noticeable expansion can be observed from the lift-off area to collapse, indicating that saccharides participate in and disrupt the monolayer structure, and implying a degree of complexity and heterogeneous distribution of species in the interfacial region. De Vasquez et al. (2022) also demonstrated that glucuronate interacts with and expands the stearic acid monolayer. Furthermore, they suggested that glucuronate intercalates into the stearic acid monolayer and leads to monolayer reorganization. Spectral evidence is needed to further clarify whether intercalation occurs in our study.

More surprisingly, we observed that the isotherms of the two saccharide matrices do not exhibit much difference at the concentrations of 0.5 and 1.0 g L^{-1}. When the saccharide concentration keeps increasing to 5.0 g L^{-1}, the molecular packing density on the interface decreases, and the apparent molecular area increases. In the presence of glucose and trehalose, the lift-off areas increased by 9 and 10 $Å^2$, respectively. Another distinguishing feature of the fatty acid isotherms is the change of slope above $\sim$ 40 mN m^{-1}. This result could be interpreted as the saccharide being "squeezed" out of the insoluble film, resulting in higher monolayer compressibility. By squeezing saccharide molecules out of the monolayer, the isotherms at a high surface pressure behave similarly to other isotherms with low saccharide concentrations. The difference is that with the increase of structural complexity of saccharides, the effect of trehalose at the same concentration is more prominent. The α, α, 1, 1 linkage between two glucose subunits in trehalose is considered to provide an elastic and rigid balance, thus allowing for strong interactions with multiple fatty acids (Clark et al., 2015). As a result, trehalose binds more readily to lipid monolayer surfaces than glucose, as is evident from experimental observations. This is consistent with the result of Crowe et al. (1984) on the effect of saccharides (glucose and trehalose) on the properties of 1,2-dimyristoyl-*sn*-glycero-3-phosphocholine (DMPC) and 1,2-dipalmitoyl-*sn*-glycero-3-phosphocholine (DPPC) monolayers. That is, the area per lipid increases with the increase of saccharide concentration, and trehalose provides the largest lateral monolayer expansion (Crowe et al., 1984). The expansion effect promoted by soluble saccharides is more relevant at lower surface pressure when alkyl chains are farther apart from each other. Clarifying and refining the interaction mechanisms by which lipid molecules interact with saccharides is critical to any attempt to model such chemical phenomena occurring at environmentally relevant interfaces.

3.4 Effect of soluble saccharides on the interfacial structure of mixed monolayers

PM-IRRAS is a surface sensitive technique that allows further study of the possible effects of soluble saccharides on lipid interfacial organization at the molecular level. Figure 5 shows the IRRAS spectra for mixed fatty acid monolayers at two different saccharides containing subphases at a surface pressure of $\sim$ 30 mN m^{-1} to ensure complete monolayer formation. Figure S4 shows the IRRAS spectra of mixed fatty acids measured at different surface pressures. It can be observed that with the increase of surface pressure, the intensity of the peaks also increases accordingly, reaching a relatively stable level around 30 mN m^{-1}. Considering the stability of the monolayer, this surface pressure was chosen to obtain the desired infrared spectra.

The absorption band in the 3000–2800 cm^{-1} region shown in Fig. 5 is ascribed to the CH stretching vibration of the alkyl chain. The main features at $\sim$ 2916 and $\sim$ 2850 cm^{-1} are related to antisymmetric ($\nu_{as}(CH_2)$) and symmetric ($\nu_s(CH_2)$) stretching modes of methylene of mixed fatty acids, respectively. The $\nu_{as}(CH_2)$ feature consistently remains stronger than $\nu_s(CH_2)$ with the increase of glucose and trehalose concentrations. These two band positions are often used empirically correlated with the order and organization within the alkyl monolayer adsorbed to the water interface, with higher wavenumbers corresponding to disordered gauche conformers. Conversely, low wavenumbers indicate that the alkyl chain of lipids is well ordered with preferential all-trans characteristics. Additionally, we also showed the wavenumbers, reflectance–absorbance intensities, peak areas, and full width at half maximum (FWHM, cm^{-1}) values of each fitted peak in Table S2. In this work, the relatively low frequencies of $\nu_{as}(CH_2)$ (2916–2918 cm^{-1}) and $\nu_s(CH_2)$ (2848–2851 cm^{-1}) hint that the molecular conformation of the fatty acid alkyl chains is dominated by the highly ordered all-trans conformation (Li et al., 2019). Despite the concentration range of saccharides varying widely, the positions of $\nu_{as}(CH_2)$ and $\nu_s(CH_2)$ showed modest sensitivity to shifts, suggesting very minor changes in the conformation of the alkyl chain. The relative weak antisymmetric ($\upsilon_{as}(CH_3)$) and symmetric methyl stretching ($\upsilon_s(CH_3)$) vibrations were observed at $\sim$ 2958 and $\sim$ 2880 cm^{-1}, respectively. These results indicate that the penetration of soluble saccharides is only superficial (along the lipid surface) and has little effect on the alkyl tail arrangement. Therefore, it is further deduced that the stabilization mechanism between saccharides and fatty acid molecules may occur in the headgroup region.

Carboxylic acids possess one hydrogen bond donor (hydroxyl) and one hydrogen bond acceptor (carbonyl) within the same functional group, the carboxyl group. The carbonyl stretching modes (υ(C=O)) of the carboxyl group at $\sim$ 1734 cm^{-1} (unhydrogen bonded), 1725 cm^{-1} (singly hydrogen bonded), and 1708 cm^{-1} (doubly hydrogen bonded) were observed in seawater (Gericke and Huhnerfuss, 1993),

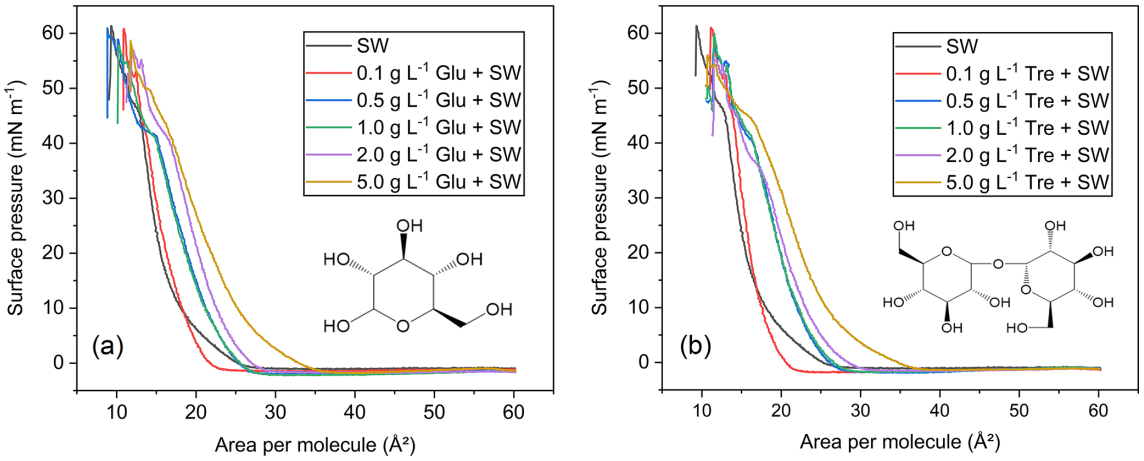

Figure 4. π-A isotherms of mixed fatty acids in the SW subphase with several concentration gradients of **(a)** glucose and **(b)** trehalose. The inset shows the molecular structures of glucose and trehalose.

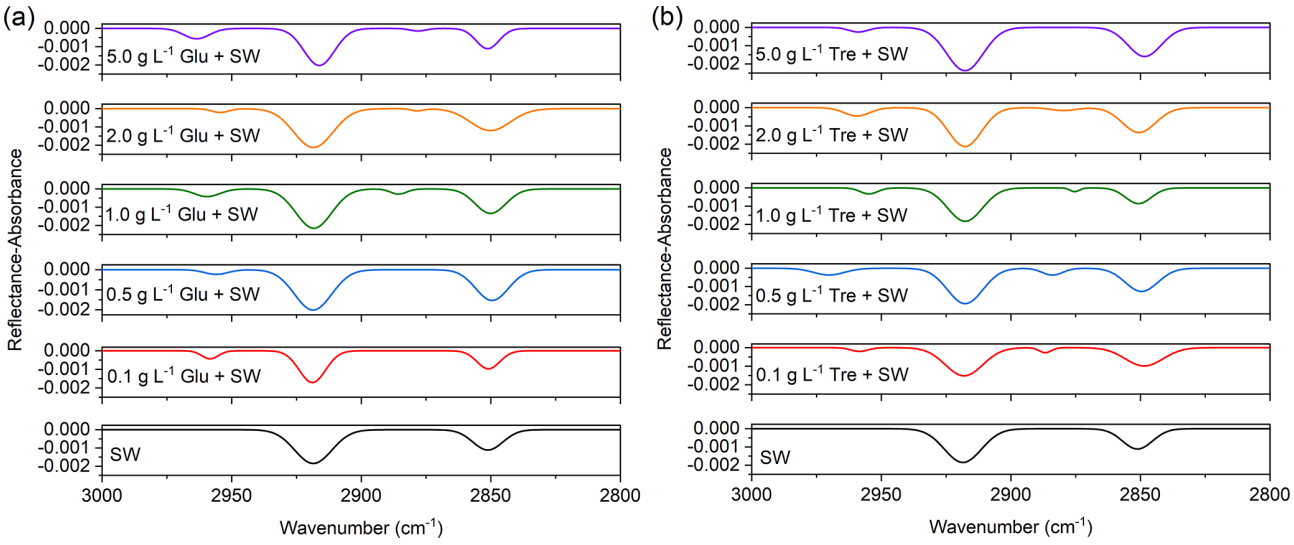

Figure 5. PM-IRRAS spectra (3000–2800 cm^{-1}) of mixed fatty acids at the air/seawater interface at different **(a)** glucose and **(b)** trehalose concentrations in the subphase.

with the strength at 1734 cm^{-1} being the highest (Fig. 6). This band component at 1734 cm^{-1} is put down to the conformation with the carbonyl group almost parallel to the water surface, and the hydroxyl group is oriented toward the water surface, which is not conducive to the formation of the hydrogen bond with water subphase (Muro et al., 2010). For saccharide concentrations ranging from 0.1 to 2 g L^{-1}, the unhydrated C=O band was observed to be depressed, and the singly and doubly hydrogen-bonded carbonyl components at $\sim$ 1720 and $\sim$ 1708 cm^{-1} became dominant (Johann et al., 2001). At the highest glucose concentration, the Langmuir model appears to capture a saturation effect, where the establishment of hydrogen bonds is associated with a strong initial increase in glucose organic enrichment, followed by surface saturation at higher organic concentration. We also displayed the wavenumbers, reflectance–absorbance intensities, peak areas, and full width at half maximum (FWHM, cm^{-1}) values of each fitted peak in the region of 1800–1300 cm^{-1} in Table S3. The presence of hydrogen bonds between saccharides and the carbonyls of fatty acids is well correlated with the observed shifts in the infrared absorption band of carbonyl groups. Using FTIR experiments, Luzardo et al. (2000) showed that trehalose shifts the vibrational frequency of the carbonyl group to a lower value, which is evidence of the existence of direct hydrogen bonding between trehalose and lipid carbonyl groups. We believe that saccharides displace water surrounding the fatty acid polar headgroups and interact strongly with lipid headgroups, resulting in a slight decrease in hydration near the monolayer interface.

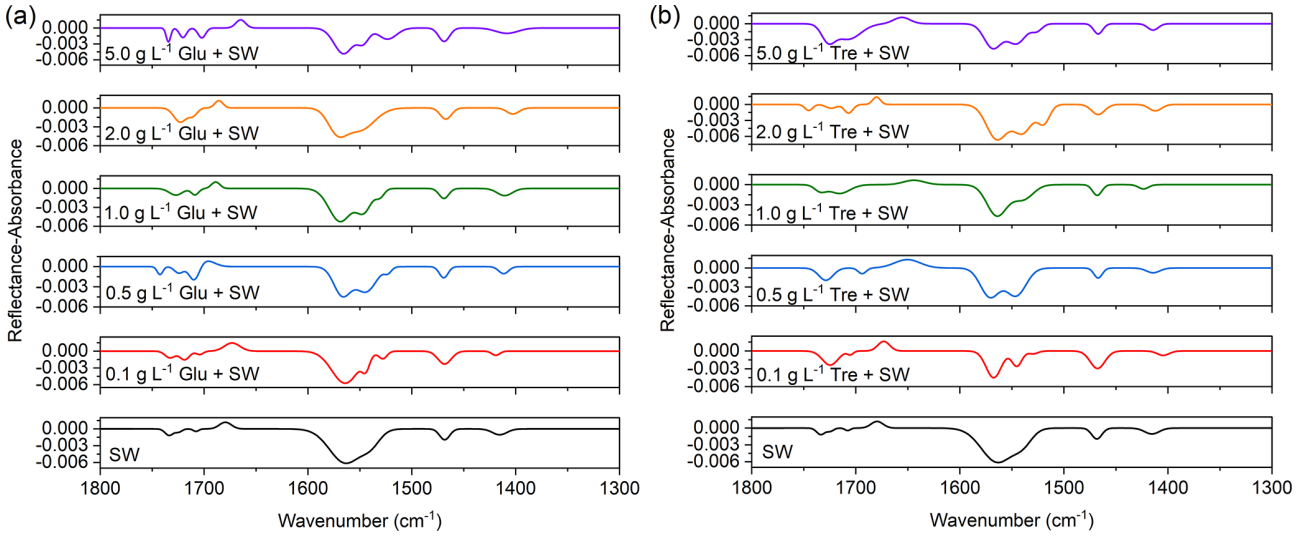

Figure 6. PM-IRRAS spectra (1800–1300 cm^{-1}) of mixed fatty acids at the air/seawater interface at different **(a)** glucose and **(b)** trehalose concentrations in the subphase.

The non-monotonic hydrogen bond strength shows that the interaction at the interface manifests as competing contributions that dominate at different concentrations. Within the concentration range studied, saccharides tend to "displace" water, creating unique environments. In some recent studies, this "water displacement" hypothesis was supported by molecular dynamics (MD) simulations, fluorescence microscopy, and nuclear magnetic resonance (NMR) (Lambruschini et al., 2000; You et al., 2021; Kapla et al., 2015). Previous MD simulation studies showed that the hydrogen bond lifetime between trehalose and membrane was longer than that established between water and membrane (Villarreal et al., 2004). This is because water molecules are more mobile and can exchange more frequently at the interface than trehalose. Another study also confirmed that sugar–lipid hydrogen bonds are stronger than water–lipid hydrogen bonds due to low endothermicity, and they remain largely intact even at very high sugar concentrations (You et al., 2021). During SSA production, the bubbles remain on the surface for a period of time during which the bubble's film cap is expelled (Modini et al., 2013), and water and soluble molecules are removed from the bubble film, a process that is thought to be important for the high organic matter fraction. These experiments suggest that there are strong hydrogen bonds between saccharides and fatty acid molecules, so that saccharide molecules may still be bound to the fatty acid monolayer and not be washed out as the film cap drains.

Long chain fatty acid amphiphiles that spread as a monolayer on the alkaline subphase undergo dissociation. The ratio of neutral fatty acids and ionized carboxylates in the monolayer depends on the pH of the subphase solution. At natural oceanic conditions (pH $\sim$ 8.1), deprotonation of the carboxylic acid groups results in two carboxylate stretches. The broad and strong antisymmetric carboxylate stretch (υ_{as}(COO)) was observed at $\sim$ 1564 cm^{-1}, and the symmetric carboxylate stretch (υ_{s}(COO)) at $\sim$ 1415 cm^{-1}. The presence of salt in seawater caused the υ_{as}(COO) to split into three peaks at $\sim$ 1564, $\sim$ 1544, and $\sim$ 1528 cm^{-1}. Additionally, we found a shift in the major carboxylate stretching mode from 1564 to higher frequency at $\sim$ 1572 cm^{-1}, which may be indicative of carboxylate dehydration upon interactions with saccharides. Another distinctive feature in all spectra obtained at $\sim$ 1469 cm^{-1} was assigned to the CH_2 scissoring vibration ($\delta(CH_2)$) of the aliphatic chain (Muro et al., 2010). This wavenumber value somewhat indicates an orthorhombic subcell structure. It should be noted that the $\delta(CH_2)$ vibrational position for the surface membrane of the mixed fatty acids reported here is relatively insensitive to saccharides and their concentrations. This observation confirms the conclusions drawn from the $\nu_{as}(CH_2)$ and $\nu_{s}(CH_2)$ wavenumbers that higher alkyl chain conformational orders are obtained either on the surface of pure seawater or on subphases containing glucose or trehalose.

3.5 Effect of soluble saccharides on particle morphology

Particle morphology can affect the surface composition, heterogeneous chemistry, gas-particle partitioning of semivolatile organics, and water uptake of aerosols (Unger et al., 2020; Ruehl et al., 2016; Lee et al., 2021). We examined the particle morphology and qualitatively compared SSAs between different model systems, including the mixed effects of saccharides and fatty acids. Compared to the study by Unger et al. (2020), the samples we investigated had compositions that were closely connected to the chemical composition of sea spray aerosols.

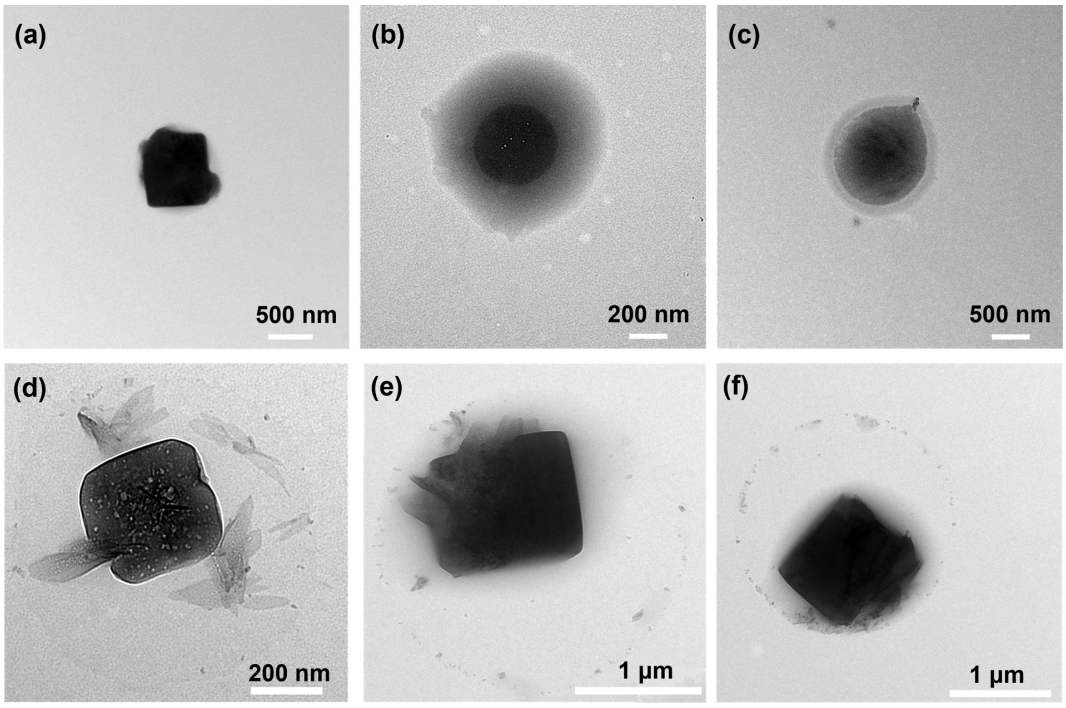

Figure 7. TEM images of morphology identified for sea spray aerosols produced from **(a)** natural seawater, **(b)** seawater with glucose, and **(c)** seawater with trehalose without fatty acids organic layer, **(d)** natural seawater with fatty acids, **(e)** seawater with glucose and fatty acids, and **(f)** seawater with trehalose and fatty acids.

Figure 7 depicts TEM images of SSA particles generated by the plunging jet sea spray aerosol generator, which can provide clues about how saccharide and/or fatty acid components are interacting with sea salt. As can be seen from Fig. 7a, SSA produced from pure natural seawater by the plunging jet exhibited a prism-like morphology that is predominantly inorganic in nature (Lee et al., 2020). This standard cubic shape also suggests that NaCl is an important component of the natural seawater sample used in this study. The morphology of SSA particles was strongly affected by the incorporation of saccharides. In the presence of saccharides, the images indicate that these SSA particles exhibit a core–shell morphology with the shell portion being mainly organic in composition, whereas the sea salt cores are more spherical in nature, demonstrating that organic substances inhibit the cubic crystallization of NaCl. The core–shell morphologies adopted here are congruent with previous studies on the NaCl/glucose binary system and authentic SSA samples observed using atomic force microscopy (Ray et al., 2019; Estillore et al., 2017). However, as shown in Fig. 7d–f, the presence of the fatty acid layer on the surface not only reduces the number concentration of SSA produced but also tends to maintain the cubic shape of the core of SSA. When fatty acids and saccharides coexist, we can still observe the preservation of the core–shell structure. In brief, the results presented in this study suggest that the heterogeneity within a particle type is a function of seawater chemistry.

3.6 Proposed mechanism for bulk saccharide transfer to SSA

The molecular level interactions between small saccharides and fatty acids discussed in previous sections can be summarized using the model presented in Fig. 8. Aqueous aerosols coated by surface-active organic matter (Fig. 8a), such as SSA, generally hold inverse micelle structures with hydrophilic headgroups pointing toward the aqueous phase and hydrophobic tails pointing toward the gas phase (Blackshaw et al., 2019). At the center of the inverse micelle, a water pool is formed that can dissolve polar substances such as saccharides, proteins, enzymes, amino acids, and nucleic acid. This unique physico-chemical environment may enhance the possibility of saccharides transfer to SSA. Through the Langmuir surface pressure–area experiment combined with infrared reflection–absorption spectroscopy, we initially explored the possible mechanism of the transfer of saccharides at the air/water interface. In a nutshell, we infer that saccharides initially in the aqueous phase move steadily to the interface and act as a substituent for water molecules and are located in the headgroup region of the fatty acids. During the binding process, the saccharides displace the oriented water molecules that are bound to the fatty acids through hydrogen bonds, establishing new hydrogen bonds with the carbonyl group of fatty acids (You et al., 2021).

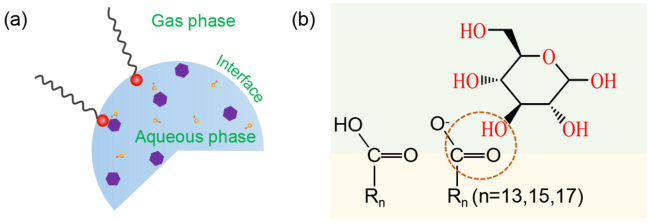

Figure 8. **(a)** Proposed model of fatty acid–saccharide interaction at the air/water interface. **(b)** Description of possible mechanisms of fatty acid–saccharide interaction at the air/water interface.

3.7 Atmospheric implications

Despite extensive efforts, the exhaustive relationships between ocean organic carbon pools and the chemical composition of SSAs are still outstanding. The coupling of this sea spray aerosol simulation generator with the interfacial monolayer model lays the foundation for further studies of the material relationship between the ocean and SSA. The research reported here yielded two key findings. First, SSA production and particle size distribution are usually extremely sensitive to organic matter, and small saccharides dissolved in seawater are critical to the formation, size, and composition of SSA. Our results strongly support that those saccharides can greatly promote the generation of SSA particles and make SSA show core–shell morphology characteristics. A previous study revealed that the SSA number concentration in coastal samples was inversely correlated with salinity, with several organic tracers, including dissolved and chromophoric organic carbon (DOC, CDOM), marine microgels, and chlorophyll *a* (Chl-*a*) being positively correlated but not associated with viral and bacterial abundances (Park et al., 2019). However, it is more complex in the real-world environment where the influencing factors are compounded. Other limitations to this study include the limited representation, by the simple chemical structural models, of the myriad complex biomolecules that exist in the ocean, spanning dissolved, colloidal, and particulate matter. It is recommended that future studies targeting the production and property of SSA include the effects of different types of organic matter to determine whether they fully mimic the arrays of SSA particles and include more complete organic matter systems as well as biological species.

Second, it has been suggested that the abundant organic content in SSA plays a key role in determining cloud condensation nucleation and ice nucleating activity (O'Dowd et al., 2004). Therefore, climate models demand a predictive representation of SSA chemical composition to accurately simulate climate processes in the marine boundary layer (Burrows et al., 2016; Bertram et al., 2018). However, the source of organic enrichment observed in SSA remains speculative, which poses challenges to the modeling of the aerosol impact on atmospheric chemistry and climate science. A recent study has raised that the cooperative adsorption of saccharides with insoluble lipid monolayers may make important contributions to the sea spray aerosols and even have climatic consequences with broad research prospects (Burrows et al., 2014). Their team recently developed a process model for understanding the feedback relationship between marine biology, sea spray organic matter, and climate, called OCEANFILMS (Organic Compounds from Ecosystems to Aerosols: Natural Films and Interfaces via Langmuir Molecular Surfactants) sea spray organic aerosol emissions – implementation in a global climate model and impacts on clouds (Burrows et al., 2022). In this work, we used the Langmuir monolayer to model possible interactions between subphase soluble saccharides and surface fatty acid molecules. A subsequent study used infrared reflection–absorption spectroscopy to determine the interaction mechanism between two simple soluble saccharides and tightly packed fatty acids monolayers at the air/water interface. Combining the above experimental results, we infer that the hydrogen bonding interaction between saccharides and the carbonyl group of surface insoluble fatty acid molecules contributes to its transfer from the ocean to the atmosphere. At present, this mechanism of saccharides transfer and enrichment has not been emphasized in the model describing SSA formation. Furthermore, our results may be an effective complement and development to OCEANFILMS model theory, and by adding the chemical interaction between soluble saccharides and an insoluble fatty acid surfactant monolayer, the consistency of modeled sea spray chemistry with observed marine aerosol chemistry may be improved. To further examine the feasibility of the hydrogen bonding mechanism as an interfacial organic enrichment mechanism, it is necessary to further explore and verify the interaction of other carbohydrates with common surface-insoluble molecules in future studies.

4 Conclusions

In summary, we simulated the production of SSA in natural seawater spiked with two common soluble saccharides using a plunging water jet generator, and we revealed the possible mechanism of saccharide transfer from bulk seawater into SSA combined with surface-sensitive infrared spectroscopy techniques. We confirmed that glucose and trehalose can significantly promote the production of SSA and alter the surface morphology of SSA particles. This highlights the potential for a direct oceanic source of carbohydrate organics through bubble bursting. In addition, trehalose showed stronger promoting ability than glucose, while the surface fatty acid layer played an inhibitory role. Using the mixture of saturated fatty acids MA, PA, and SA as the proxy of SSA surface film, the π-A isotherms provided strong evidence that saccharides can interact with insoluble fatty acid monolayers and be adsorbed at the monolayer, which caused expansion of the monolayer and made the films heterogeneous. According to the IRRAS spectra, soluble saccharides did not

produce a significant impact on the order of fatty acid alkyl chains. We further infer that soluble saccharides are mainly located on the subsurface below the monolayer and interact with carbonyl groups of fatty acids by forming hydrogen bonds to facilitate their sea–air transfer. Crucially, this work provides physical and molecular signatures of potentially important saccharides transfer mechanisms with general implications for understanding how saccharide–lipid interactions affect sea spray aerosol systems for real-world scenarios.

Data availability. Experimental data are available upon request to the corresponding author.

Supplement. The supplement related to this article is available online at: https://doi.org/10.5194/acp-23-2235-2023-supplement.

Author contributions. MX: conceived the experiment, data curation, formal analysis, writing original draft, and writing – review and editing. NTT: writing – review and editing. JL: writing – review and editing. LD: supervision, conceived the experiment, funding acquisition, and writing – review and editing.

Competing interests. The contact author has declared that none of the authors has any competing interests.

Disclaimer. Publisher's note: Copernicus Publications remains neutral with regard to jurisdictional claims in published maps and institutional affiliations.

Special issue statement. This article is part of the special issue "Marine organic matter: from biological production in the ocean to organic aerosol particles and marine clouds (ACP/OS inter-journal SI)". It is not associated with a conference.

Acknowledgements. We would like to thank Xiaoju Li from State Key Laboratory of Microbial Technology, Shandong University, for help and guidance in TEM.

Financial support. This research has been supported by the National Natural Science Foundation of China (grant nos. 22076099 and 21876098), the Department of Education of Shandong Province (grant no. 2019KJD007), and the Fundamental Research Fund of Shandong University (grant no. 2020QNQT012).

Review statement. This paper was edited by Manuela van Pinxteren and reviewed by Kimberly Carter-Fenk and two anonymous referees.

References

Bertram, T. H., Cochran, R. E., Grassian, V. H., and Stone, E. A.: Sea spray aerosol chemical composition: Elemental and molecular mimics for laboratory studies of heterogeneous and multiphase reactions, Chem. Soc. Rev., 47, 2374–2400, https://doi.org/10.1039/c7cs00008a, 2018.

Blackshaw, K. J., Varmecky, M. G., and Patterson, J. D.: Interfacial structure and partitioning of nitrate ions in reverse micelles, J. Phys. Chem. A, 123, 336–342, https://doi.org/10.1021/acs.jpca.8b09751, 2019.

Brooks, S. D. and Thornton, D. C. O.: Marine aerosols and clouds, Annu. Rev. Mar. Sci., 10, 289–313, https://doi.org/10.1146/annurev-marine-121916-063148, 2018.

Burrows, S. M., Ogunro, O., Frossard, A. A., Russell, L. M., Rasch, P. J., and Elliott, S. M.: A physically based framework for modeling the organic fractionation of sea spray aerosol from bubble film Langmuir equilibria, Atmos. Chem. Phys., 14, 13601–13629, https://doi.org/10.5194/acp-14-13601-2014, 2014.

Burrows, S. M., Gobrogge, E., Fu, L., Link, K., Elliott, S. M., Wang, H. F., and Walker, R.: OCEANFILMS-2: Representing coadsorption of saccharides in marine films and potential impacts on modeled marine aerosol chemistry, Geophys. Res. Lett., 43, 8306–8313, https://doi.org/10.1002/2016gl069070, 2016.

Burrows, S. M., Easter, R. C., Liu, X., Ma, P.-L., Wang, H., Elliott, S. M., Singh, B., Zhang, K., and Rasch, P. J.: OCEANFILMS (Organic Compounds from Ecosystems to Aerosols: Natural Films and Interfaces via Langmuir Molecular Surfactants) sea spray organic aerosol emissions – implementation in a global climate model and impacts on clouds, Atmos. Chem. Phys., 22, 5223–5251, https://doi.org/10.5194/acp-22-5223-2022, 2022.

Carter-Fenk, K. A. and Allen, H. C.: Collapse mechanisms of nascent and aged sea spray aerosol proxy films, Atmosphere, 9, 503, https://doi.org/10.3390/atmos9120503, 2018.

Christiansen, S., Salter, M. E., Gorokhova, E., Nguyen, Q. T., and Bilde, M.: Sea spray aerosol formation: Laboratory results on the role of air entrainment, water temperature and phytoplankton biomass, Environ. Sci. Technol., 53, 13107–13116, https://doi.org/10.1021/acs.est.9b04078, 2019.

Clark, G. A., Henderson, J. M., Heffern, C., Akgun, B., Majewski, J., and Lee, K. Y. C.: Synergistic interactions of sugars/polyols and monovalent salts with phospholipids depend upon sugar/polyol complexity and anion identity, Langmuir, 31, 12688–12698, https://doi.org/10.1021/acs.langmuir.5b02815, 2015.

Cochran, R. E., Laskina, O., Jayarathne, T., Laskin, A., Laskin, J., Lin, P., Sultana, C., Lee, C., Moore, K. A., Cappa, C. D., Bertram, T. H., Prather, K. A., Grassian, V. H., and Stone, E. A.: Analysis of organic anionic surfactants in fine and coarse fractions of freshly emitted sea spray aerosol, Environ. Sci. Technol., 50, 2477–2486, https://doi.org/10.1021/acs.est.5b04053, 2016.

Cochran, R. E., Laskina, O., Trueblood, J. V., Estillore, A. D., Morris, H. S., Jayarathne, T., Sultana, C. M., Lee, C., Lin, P., Laskin, J., Laskin, A., Dowling, J. A., Qin, Z., Cappa, C. D., Bertram, T. H., Tivanski, A. V., Stone, E. A., Prather, K. A., and Grassian, V. H.: Molecular diversity of sea spray aerosol particles: Impact of ocean biology on particle composition and hygroscopicity, Chem, 2, 655–667, https://doi.org/10.1016/j.chempr.2017.03.007, 2017.

Cravigan, L. T., Mallet, M. D., Vaattovaara, P., Harvey, M. J., Law, C. S., Modini, R. L., Russell, L. M., Stelcer, E., Cohen, D. D., Olsen, G., Safi, K., Burrell, T. J., and Ristovski, Z.: Sea spray aerosol organic enrichment, water uptake and surface tension effects, Atmos. Chem. Phys., 20, 7955–7977, https://doi.org/10.5194/acp-20-7955-2020, 2020.

Crowe, J. H., Whittam, M. A., Chapman, D., and Crowe, L. M.: Interactions of phospholipid monolayers with carbohydrates, Biochim. Biophys. Acta, 769, 151–159, https://doi.org/10.1016/0005-2736(84)90018-x, 1984.

Cunliffe, M., Engel, A., Frka, S., Gašparović, B., Guitart, C., Murrell, J. C., Salter, M., Stolle, C., Upstill-Goddard, R., and Wurl, O.: Sea surface microlayers: A unified physicochemical and biological perspective of the air–ocean interface, Prog. Oceanogr., 109, 104–116, https://doi.org/10.1016/j.pocean.2012.08.004, 2013.

Deane, G. B. and Stokes, M. D.: Scale dependence of bubble creation mechanisms in breaking waves, Nature, 418, 839–844, https://doi.org/10.1038/nature00967, 2002.

de Vasquez, M. G. V., Rogers, M. M., Carter-Fenk, K. A., and Allen, H. C.: Discerning poly- and monosaccharide enrichment mechanisms: Alginate and glucuronate adsorption to a stearic acid sea surface microlayer, ACS Earth Space Chem., 6, 1581–1595, https://doi.org/10.1021/acsearthspacechem.2c00066, 2022.

Elliott, S., Burrows, S. M., Deal, C., Liu, X., Long, M., Ogunro, O., Russell, L. M., and Wingenter, O.: Prospects for simulating macromolecular surfactant chemistry at the ocean-atmosphere boundary, Environ. Res. Lett., 9, 064012, https://doi.org/10.1088/1748-9326/9/6/064012, 2014.

Estillore, A. D., Morris, H. S., Or, V. W., Lee, H. D., Alves, M. R., Marciano, M. A., Laskina, O., Qin, Z., Tivanski, A. V., and Grassian, V. H.: Linking hygroscopicity and the surface microstructure of model inorganic salts, simple and complex carbohydrates, and authentic sea spray aerosol particles, Phys. Chem. Chem. Phys., 19, 21101–21111, https://doi.org/10.1039/c7cp04051b, 2017.

Facchini, M. C., Rinaldi, M., Decesari, S., Carbone, C., Finessi, E., Mircea, M., Fuzzi, S., Ceburnis, D., Flanagan, R., Nilsson, E. D., de Leeuw, G., Martino, M., Woeltjen, J., and O'Dowd, C. D.: Primary submicron marine aerosol dominated by insoluble organic colloids and aggregates, Geophys. Res. Lett., 35, L17814, https://doi.org/10.1029/2008gl034210, 2008.

Frossard, A. A., Russell, L. M., Burrows, S. M., Elliott, S. M., Bates, T. S., and Quinn, P. K.: Sources and composition of submicron organic mass in marine aerosol particles, J. Geophys. Res.-Atmos., 119, 12977–13003, https://doi.org/10.1002/2014jd021913, 2014.

Fuentes, E., Coe, H., Green, D., de Leeuw, G., and McFiggans, G.: Laboratory-generated primary marine aerosol via bubble-bursting and atomization, Atmos. Meas. Tech., 3, 141–162, https://doi.org/10.5194/amt-3-141-2010, 2010.

Gericke, A. and Huhnerfuss, H.: In-situ investigation of saturated long-chain fatty-acids at the air-water interface by external Infrared reflection-absorption spectrometry, J. Phys. Chem., 97, 12899–12908, https://doi.org/10.1021/j100151a044, 1993.

Hasenecz, E. S., Kaluarachchi, C. P., Lee, H. D., Tivanski, A. V., and Stone, E. A.: Saccharide transfer to sea spray aerosol enhanced by surface activity, calcium, and protein interactions, ACS Earth Space Chem., 3, 2539–2548, https://doi.org/10.1021/acsearthspacechem.9b00197, 2019.

Hasenecz, E. S., Jayarathne, T., Pendergraft, M. A., Santander, M. V., Mayer, K. J., Sauer, J., Lee, C., Gibson, W. S., Kruse, S. M., Malfatti, F., Prather, K. A., and Stone, E. A.: Marine bacteria affect saccharide enrichment in sea spray aerosol during a phytoplankton bloom, ACS Earth Space Chem., 4, 1638–1649, https://doi.org/10.1021/acsearthspacechem.0c00167, 2020.

Hawkins, L. N. and Russell, L.: Polysaccharides, proteins, and phytoplankton fragments: Four chemically distinct types of marine primary organic aerosol classified by single particle spectromicroscopy, Adv. Meteorol., 2010, 612132, https://doi.org/10.1155/2010/612132, 2010.

Hultin, K. A. H., Nilsson, E. D., Krejci, R., Martensson, E. M., Ehn, M., Hagstrom, A., and de Leeuw, G.: In situ laboratory sea spray production during the Marine Aerosol Production 2006 cruise on the northeastern Atlantic Ocean, J. Geophys. Res.-Atmos., 115, D06201, https://doi.org/10.1029/2009jd012522, 2010.

Johann, R., Vollhardt, D., and Mohwald, H.: Study of the pH dependence of head group bonding in arachidic acid monolayers by polarization modulation infrared reflection absorption spectroscopy, Colloid. Surface. A, 182, 311–320, https://doi.org/10.1016/s0927-7757(00)00812-8, 2001.

Kapla, J., Engstrom, O., Stevensson, B., Wohlert, J., Widmalm, G., and Maliniak, A.: Molecular dynamics simulations and NMR spectroscopy studies of trehalose-lipid bilayer systems, Phys. Chem. Chem. Phys., 17, 22438–22447, https://doi.org/10.1039/c5cp02472b, 2015.

King, S. M., Butcher, A. C., Rosenoern, T., Coz, E., Lieke, K. I., de Leeuw, G., Nilsson, E. D., and Bilde, M.: Investigating primary marine aerosol properties: CCN activity of sea salt and mixed inorganic-organic particles, Environ. Sci. Technol., 46, 10405–10412, https://doi.org/10.1021/es300574u, 2012.

Lambruschini, C., Relini, A., Ridi, A., Cordone, L., and Gliozzi, A.: Trehalose interacts with phospholipid polar heads in Langmuir monolayers, Langmuir, 16, 5467–5470, https://doi.org/10.1021/la991641e, 2000.

Lee, C., Dommer, A. C., Schiffer, J. M., Amaro, R. E., Grassian, V. H., and Prather, K. A.: Cation-driven lipopolysaccharide morphological changes impact heterogeneous reactions of nitric acid with sea spray aerosol particles, J. Phys. Chem. Lett., 12, 5023–5029, https://doi.org/10.1021/acs.jpclett.1c00810, 2021.

Lee, H. D., Wigley, S., Lee, C., Or, V. W., Hasenecz, E. S., Stone, E. A., Grassian, V. H., Prather, K. A., and Tivanski, A. V.: Physicochemical mixing state of sea spray aerosols: Morphologies exhibit size dependence, ACS Earth Space Chem., 4, 1604–1611, https://doi.org/10.1021/acsearthspacechem.0c00153, 2020.

Lee, K. Y. C.: Collapse mechanisms of Langmuir monolayers, Annu. Rev. Phys. Chem., 59, 771–791, https://doi.org/10.1146/annurev.physchem.58.032806.104619, 2008.

Li, S., Jiang, X., Roveretto, M., George, C., Liu, L., Jiang, W., Zhang, Q., Wang, W., Ge, M., and Du, L.: Photochemical aging of atmospherically reactive organic compounds involving brown carbon at the air–aqueous interface, Atmos. Chem. Phys., 19, 9887–9902, https://doi.org/10.5194/acp-19-9887-2019, 2019.

Link, K. A., Spurzem, G. N., Tuladhar, A., Chase, Z., Wang, Z. M., Wang, H. F., and Walker, R. A.: Cooperative adsorption of trehalose to DPPC monolayers at the water-air interface stud-

ied with vibrational sum frequency generation, J. Phys. Chem. B, 123, 8931–8938, https://doi.org/10.1021/acs.jpcb.9b07770, 2019a.

Link, K. A., Spurzem, G. N., Tuladhar, A., Chase, Z., Wang, Z. M., Wang, H. F., and Walker, R. A.: Organic enrichment at aqueous interfaces: Cooperative adsorption of glucuronic acid to DPPC monolayers studied with vibrational sum frequency generation, J. Phys. Chem. A, 123, 5621–5632, https://doi.org/10.1021/acs.jpca.9b02255, 2019b.

Liu, L. R., Du, L., Xu, L., Li, J. L., and Tsona, N. T.: Molecular size of surfactants affects their degree of enrichment in the sea spray aerosol formation, Environ. Res., 206, 112555, https://doi.org/10.1016/j.envres.2021.112555, 2022.

Luzardo, M. D., Amalfa, F., Nunez, A. M., Diaz, S., de Lopez, A. C. B., and Disalvo, E. A.: Effect of trehalose and sucrose on the hydration and dipole potential of lipid bilayers, Biophys. J., 78, 2452–2458, https://doi.org/10.1016/s0006-3495(00)76789-0, 2000.

Lv, C., Tsona, N. T., and Du, L.: Sea spray aerosol formation: Results on the role of different parameters and organic concentrations from bubble bursting experiments, Chemosphere, 252, 126456, https://doi.org/10.1016/j.chemosphere.2020.126456, 2020.

Modini, R. L., Russell, L. M., Deane, G. B., and Stokes, M. D.: Effect of soluble surfactant on bubble persistence and bubble-produced aerosol particles, J. Geophys. Res.-Atmos., 118, 1388–1400, https://doi.org/10.1002/jgrd.50186, 2013.

Muro, M., Itoh, Y., and Hasegawa, T.: A conformation and orientation model of the carboxylic group of fatty acids dependent on chain length in a Langmuir monolayer film studied by polarization-modulation infrared reflection absorption spectroscopy, J. Phys. Chem. B, 114, 11496–11501, https://doi.org/10.1021/jp105862q, 2010.

O'Dowd, C. D., Facchini, M. C., Cavalli, F., Ceburnis, D., Mircea, M., Decesari, S., Fuzzi, S., Yoon, Y. J., and Putaud, J. P.: Biogenically driven organic contribution to marine aerosol, Nature, 431, 676–680, https://doi.org/10.1038/nature02959, 2004.

Pakulski, J. D. and Benner, R.: An improved method for the hydrolysis and MBTH analysis of dissolved and particulate carbohydrates in seawater, Mar. Chem., 40, 143–160, https://doi.org/10.1016/0304-4203(92)90020-B, 1992.

Park, J., Dall'Osto, M., Park, K., Kim, J. H., Park, J., Park, K. T., Hwang, C. Y., Jang, G. I., Gim, Y., Kang, S., Park, S., Jin, Y. K., Yum, S. S., Simo, R., and Yoon, Y. J.: Arctic primary aerosol production strongly influenced by riverine organic matter, Environ. Sci. Technol., 53, 8621–8630, https://doi.org/10.1021/acs.est.9b03399, 2019.

Partanen, A.-I., Dunne, E. M., Bergman, T., Laakso, A., Kokkola, H., Ovadnevaite, J., Sogacheva, L., Baisnée, D., Sciare, J., Manders, A., O'Dowd, C., de Leeuw, G., and Korhonen, H.: Global modelling of direct and indirect effects of sea spray aerosol using a source function encapsulating wave state, Atmos. Chem. Phys., 14, 11731–11752, https://doi.org/10.5194/acp-14-11731-2014, 2014.

Pavinatto, F. J., Caseli, L., Pavinatto, A., dos Santos, D. S., Nobre, T. M., Zaniquelli, M. E. D., Silva, H. S., Miranda, P. B., and de Oliveira, O. N.: Probing chitosan and phospholipid interactions using Langmuir and Langmuir-Blodgett films as cell membrane models, Langmuir, 23, 7666–7671, https://doi.org/10.1021/la700856a, 2007.

Perkins, R. and Vaida, V.: Phenylalanine increases membrane permeability, J. Am. Chem. Soc., 139, 14388–14391, https://doi.org/10.1021/jacs.7b09219, 2017.

Prather, K. A., Bertram, T. H., Grassian, V. H., Deane, G. B., Stokes, M. D., DeMott, P. J., Aluwihare, L. I., Palenik, B. P., Azam, F., Seinfeld, J. H., Moffet, R. C., Molina, M. J., Cappa, C. D., Geiger, F. M., Roberts, G. C., Russell, L. M., Ault, A. P., Baltrusaitis, J., Collins, D. B., Corrigan, C. E., Cuadra-Rodriguez, L. A., Ebben, C. J., Forestieri, S. D., Guasco, T. L., Hersey, S. P., Kim, M. J., Lambert, W. F., Modini, R. L., Mui, W., Pedler, B. E., Ruppel, M. J., Ryder, O. S., Schoepp, N. G., Sullivan, R. C., and Zhao, D. F.: Bringing the ocean into the laboratory to probe the chemical complexity of sea spray aerosol, P. Natl. Acad. Sci. USA, 110, 7550–7555, https://doi.org/10.1073/pnas.1300262110, 2013.

Quinn, P. K., Bates, T. S., Schulz, K. S., Coffman, D. J., Frossard, A. A., Russell, L. M., Keene, W. C., and Kieber, D. J.: Contribution of sea surface carbon pool to organic matter enrichment in sea spray aerosol, Nat. Geosci., 7, 228–232, https://doi.org/10.1038/ngeo2092, 2014.

Quinn, P. K., Collins, D. B., Grassian, V. H., Prather, K. A., and Bates, T. S.: Chemistry and related properties of freshly emitted sea spray aerosol, Chem. Rev., 115, 4383–4399, https://doi.org/10.1021/cr500713g, 2015.

Quinn, P. K., Coffman, D. J., Johnson, J. E., Upchurch, L. M., and Bates, T. S.: Small fraction of marine cloud condensation nuclei made up of sea spray aerosol, Nat. Geosci., 10, 674–679, https://doi.org/10.1038/ngeo3003, 2017.

Ray, K. K., Lee, H. D., Gutierrez, M. A., Chang, F. J., and Tivanski, A. V.: Correlating 3D morphology, phase state, and viscoelastic properties of individual substrate-deposited particles, Anal. Chem., 91, 7621–7630, https://doi.org/10.1021/acs.analchem.9b00333, 2019.

Ruehl, C. R., Davies, J. F., and Wilson, K. R.: An interfacial mechanism for cloud droplet formation on organic aerosols, Science, 351, 1447–1450, https://doi.org/10.1126/science.aad4889, 2016.

Russell, L. M., Hawkins, L. N., Frossard, A. A., Quinn, P. K., and Bates, T. S.: Carbohydrate-like composition of submicron atmospheric particles and their production from ocean bubble bursting, P. Natl. Acad. Sci. USA, 107, 6652–6657, https://doi.org/10.1073/pnas.0908905107, 2010.

Schill, S., Burrows, S., Hasenecz, E., Stone, E., and Bertram, T.: The impact of divalent cations on the enrichment of soluble saccharides in primary sea spray aerosol, Atmosphere, 9, 476, https://doi.org/10.3390/atmos9120476, 2018.

Schmitt-Kopplin, P., Liger-Belair, G., Koch, B. P., Flerus, R., Kattner, G., Harir, M., Kanawati, B., Lucio, M., Tziotis, D., Hertkorn, N., and Gebefügi, I.: Dissolved organic matter in sea spray: a transfer study from marine surface water to aerosols, Biogeosciences, 9, 1571–1582, https://doi.org/10.5194/bg-9-1571-2012, 2012.

Unger, I., Saak, C. M., Salter, M., Zieger, P., Patanen, M., and Bjorneholm, O.: Influence of organic acids on the surface composition of sea spray aerosol, J. Phys. Chem. A, 124, 422–429, https://doi.org/10.1021/acs.jpca.9b09710, 2020.

van Pinxteren, M., Muller, C., Iinuma, Y., Stolle, C., and Herrmann, H.: Chemical characterization of dissolved organic

compounds from coastal sea surface micro layers (Baltic Sea, Germany), Environ. Sci. Technol., 46, 10455–10462, https://doi.org/10.1021/es204492b, 2012.

van Pinxteren, M., Fomba, K. W., Triesch, N., Stolle, C., Wurl, O., Bahlmann, E., Gong, X., Voigtländer, J., Wex, H., Robinson, T.-B., Barthel, S., Zeppenfeld, S., Hoffmann, E. H., Roveretto, M., Li, C., Grosselin, B., Daële, V., Senf, F., van Pinxteren, D., Manzi, M., Zabalegui, N., Frka, S., Gašparović, B., Pereira, R., Li, T., Wen, L., Li, J., Zhu, C., Chen, H., Chen, J., Fiedler, B., von Tümpling, W., Read, K. A., Punjabi, S., Lewis, A. C., Hopkins, J. R., Carpenter, L. J., Peeken, I., Rixen, T., Schulz-Bull, D., Monge, M. E., Mellouki, A., George, C., Stratmann, F., and Herrmann, H.: Marine organic matter in the remote environment of the Cape Verde islands – an introduction and overview to the MarParCloud campaign, Atmos. Chem. Phys., 20, 6921–6951, https://doi.org/10.5194/acp-20-6921-2020, 2020.

Villarreal, M. A., Diaz, S. B., Disalvo, E. A., and Montich, G. G.: Molecular dynamics simulation study of the interaction of trehalose with lipid membranes, Langmuir, 20, 7844–7851, https://doi.org/10.1021/la049485l, 2004.

Wang, X. F., Deane, G. B., Moore, K. A., Ryder, O. S., Stokes, M. D., Beall, C. M., Collins, D. B., Santander, M. V., Burrows, S. M., Sultana, C. M., and Prather, K. A.: The role of jet and film drops in controlling the mixing state of submicron sea spray aerosol particles, P. Natl. Acad. Sci. USA, 114, 6978–6983, https://doi.org/10.1073/pnas.1702420114, 2017.

Wurl, O., Ekau, W., Landing, W. M., and Zappa, C. J.: Sea surface microlayer in a changing ocean – A perspective, Elementa. Sci. Anthrop., 5, 31, https://doi.org/10.1525/elementa.228, 2017.

Xu, M. L., Tsona, N. T., Cheng, S. M., Li, J. L., and Du, L.: Unraveling interfacial properties of organic-coated marine aerosol with lipase incorporation, Sci. Total Environ., 782, 146893, https://doi.org/10.1016/j.scitotenv.2021.146893, 2021.

Xu, W., Ovadnevaite, J., Fossum, K. N., Lin, C. S., Huang, R. J., Ceburnis, D., and O'Dowd, C.: Sea spray as an obscured source for marine cloud nuclei, Nat. Geosci., 15, 282–286, https://doi.org/10.1038/s41561-022-00917-2, 2022.

You, X., Lee, E., Xu, C., and Baiz, C. R.: Molecular mechanism of cell membrane protection by sugars: A study of interfacial H-Bond networks, J. Phys. Chem. Lett., 12, 9602–9607, https://doi.org/10.1021/acs.jpclett.1c02451, 2021.

Zeppenfeld, S., van Pinxteren, M., van Pinxteren, D., Wex, H., Berdalet, E., Vaque, D., Dall'Osto, M., and Herrmann, H.: Aerosol marine primary carbohydrates and atmospheric transformation in the Western Antarctic Peninsula, ACS Earth Space Chem., 5, 1032–1047, https://doi.org/10.1021/acsearthspacechem.0c00351, 2021.